Inorg. Chem. **2004**, *43*, 5987–5998

Mono-, Bi-, and Trinuclear Cu^{II}-Cl Containing Products Based on the Tris(2-pyridylmethyl)amine Chelate Derived from Copper(I) Complex Dechlorination Reactions of Chloroform

Baldo Lucchese,[†] Kristi J. Humphreys,[†] Dong-Heon Lee,[‡] Christopher D. Incarvito,[§] Roger D. Sommer,[§] Arnold L. Rheingold,[§,||] and Kenneth D. Karlin*,[†]

Department of Chemistry, The Johns Hopkins University, 3400 N. Charles Street, Baltimore, Maryland 21218, Department of Chemistry, Chonbuk National University, Chonju, 561-756 South Korea, and University of Delaware, Newark, Delaware 19176

Received February 26, 2004

The ligand TMPA (tris(2-pyridylmethyl)amine) and its copper complexes have played a prominent role in recent (bio)inorganic chemistry studies; the copper(I) complex $[Cu^{I}(TMPA)(CH_3CN)]^+$ possesses an extensive dioxygen reactivity, and it is also known to effect the reductive dechlorination of substrates such as dichloromethane and benzyl and allyl chlorides. In this report, we describe a set of new analogues of TMPA, ligand 6TMPAOH, binucleating Iso-DO, and trinucleating SYMM. Copper(I) complexes with these ligands and a previously described binucleating ligand DO react with chloroform, resulting in reductive dechlorination and production of $[Cu^{II}_x(L)Cl_x]^{x+}$ ($x = 1$, 2, or 3). X-ray crystal structures of $[Cu^{II}(6TMPAOH)Cl](PF_6)$, $[Cu^{II}_2(Iso\text{-}DO)Cl_2](PF_6)_2$, $[Cu^{II}_2(DO)Cl_2](PF_6)_2$, and $[Cu_3(SYMM)Cl_3](PF_6)_3$ are presented, and the compounds are also characterized by UV–vis and EPR spectroscopies as well as cyclic voltammetry. The steric influence of a pyridyl 6-substituent (in the complexes with 6TMPAOH, Iso-DO, and SYMM) on the solid state and solution structures and redox potentials are compared and contrasted to those chlorocopper(II) complexes with a pyridyl 5′-substituent (in $[Cu^{II}_2(DO)Cl_2](PF_6)_2$ and in $[Cu^{II}(TMPA)Cl]^+$). Some insights into the reductive dechlorination process have been obtained by using ^2H NMR spectroscopy in following the reaction of $[Cu_2(Iso\text{-}DO)(CH_3CN)_2](PF_6)_2$ with $CDCl_3$, in the presence or absence of a radical trap, 2,4-di-*tert*-butylphenol.

Introduction

In the study of copper(I) complex dioxygen reactivity of bioinorganic relevance, i.e., synthetic modeling for copper proteins which either reversibly bind dioxygen or effect substrate oxidation/oxygenation reactions, a prominent role has been played by $[Cu^{I}(TMPA)(CH_3CN)]^+$ (TMPA = tris-(2-pyridylmethyl)amine, see Chart 1).[1–6] For example, this cuprous complex reacts with O_2 reversibly at low temperature

Chart 1

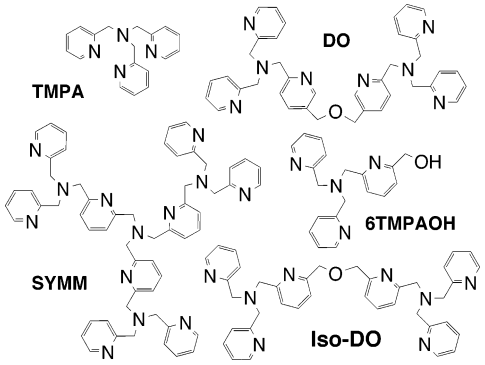

(−80 °C) first rapidly generating an initial Cu^{II}-O_2^- adduct[5] and then ultimately forming a purple colored *trans*-(μ-1,2-peroxo)dicopper(II) (end-on peroxo) complex, the first

* Author to whom correspondence should be addressed. E-mail: karlin@jhu.edu.
[†] The Johns Hopkins University.
[‡] Chonbuk National University.
[§] University of Delaware.
[||] Current address: Department of Chemistry, UC San Diego, La Jolla, CA 92093.

(1) Jacobson, R. R.; Tyeklár, Z.; Karlin, K. D.; Liu, S.; Zubieta, J. *J. Am. Chem. Soc.* **1988**, *110*, 3690−3692.
(2) Tyeklár, Z.; Jacobson, R. R.; Wei, N.; Murthy, N. N.; Zubieta, J.; Karlin, K. D. *J. Am. Chem. Soc.* **1993**, *115*, 2677−2689.
(3) Baldwin, M. J.; Ross, P. K.; Pate, J. E.; Tyeklár, Z.; Karlin, K. D.; Solomon, E. I. *J. Am. Chem. Soc.* **1991**, *113*, 8671−8679.
(4) Paul, P. P.; Tyeklár, Z.; Jacobson, R. R.; Karlin, K. D. *J. Am. Chem. Soc.* **1991**, *113*, 5322−5332.

10.1021/ic0497477 CCC: $27.50
Published on Web 08/11/2004

structurally characterized dioxygen−copper species.[3] Since then, tripodal mononuclear analogues of copper-TMPA with 6-methyl substituents,[7,8] those with varying methylene chain length between apical tertiary amine and pyridyl donor,[9] those with alkylamine group instead of pyridyl donor,[10,11] and chelates with quinolyl[12] or imdiazolyl[13] donors replacing pyridyl have also been studied for their coordination chemistry, structures, redox properties, and ligand−copper(I)/O_2 reactivity. Further, a few analogues with the tripodal tetradentate TMPA building block, but in binuclear systems, have also been studied for their coordination chemistry[14,15] and dicopper(I)/O_2 reactivity/kinetics/thermodynamics[5,16,17] as well as in reactions with DNA;[18] the latter include the ligand DO (Chart 1).

Because of the rich chemistry of TMPA and analogues, we have sought to further expand on the ligand variations and possibilities, in fact by linking two or more TMPA moieties through a 6-pyridyl (rather than 5-pyridyl group, such as in ligand DO) connection, due to the more ready accessibility of synthetic precursors. Thus, here we report on the synthesis of new ligands 6TMPAOH, Iso-DO, and SYMM (Chart 1). As will be outlined below, the reactions of copper(I) complexes with organohalides is of interest in environmental inorganic chemistry, and we previously observed that $[Cu^{II}(TMPA)Cl]^+$ forms in a reductive dehalogenation reaction of $[Cu^{I}(TMPA)(CH_3CN)]^+$ with such substrates as dichloromethane and benzyl chloride.[2,19] In this report then, we describe the synthesis of copper(I) complexes of these mono-, bi-, and trinucleating ligands 6TMPAOH, DO, Iso-DO, and SYMM. The reactions of the organohalide chloroform ($CHCl_3$) have been carried out, and in all cases corresponding $[Cu_x^{II}(L)Cl_x]^{x+}$ complexes are produced. These complexes have been characterized by X-ray diffraction and cyclic voltammetry along with UV−vis and EPR spectroscopies, and their properties are compared and contrasted, particularly with respect to the influence of the 6-pyridyl substituent present in these ligand complexes. Some mechanistic insights are also presented with respect to the $CHCl_3$ dehalogenation process.

Experimental Section

Methods and Reagents. Preparation and handling of air-sensitive materials were carried out under argon with standard Schlenk techniques or within a MBRAUN inert gas analyzer box (i.e., glovebox). Solvents and solutions were deoxygenated by either vacuum/purge cycles using argon or by bubbling argon (≈15 min) directly through the liquid. ^{1}H NMR spectra were measured in $CDCl_3$ or CD_3CN on a Bruker (300 MHz) NMR instrument, and ^{2}H NMR spectra were measured in CH_3CN on a Varian (400 MHz) instrument. All spectra were recorded in 5-mm-o.d. NMR tubes. Chemical shifts were reported as δ values downfield from internal standard Me_4Si or calibrated through the NMR solvent resonance peak. UV−visible spectral studies were carried out with a Hewlett-Packard 8453 diode array spectrometer using Agilent Technologies 95-00 software. Electron Paramagnetic Resonance (EPR) were obtained from frozen solutions at 13−16 K with 4-mm-o.d. quartz tubes in a Bruker EMX spectrometer operating at X-band utilizing microwave frequencies around 9.5 GHz. The solvent used was DMF−toluene, ≈1:1 in volume with concentrations in copper complexes at $\approx 10^{-3}$ M. The determination of $g_{\|}$, $g_{\perp}$, $A_{\|}$, and $A_{\perp}$ values was made through the use of the simulation program "*SimFonia*" provided with the Bruker EMX EPR spectrometer. Fast atomic bombardment (FAB) mass spectra were recorded at the University of Illinois at Urbana-Champaign utilizing a ZAB-SE mass spectrometer. Elemental analyses were performed at QTI (Whitehouse, NJ) or Desert Analytics (Tucson, AZ).

Reagents and solvents were of commercially available reagent quality unless otherwise stated. Acetonitrile was distilled over CaH_2. Diethyl ether was dried passing through an activated alumina column. THF was predried with solid KOH and then distilled over sodium benzophenone. Methanol was distilled over CaH_2 and deionized water was used (18.3 MΩ-cm). Prior to use bis(2-picolyl)-amine (Richman Chemical) was purified by distillation, and N-bromosuccinimide was recrystallized from deionized H_2O. All ligands were made in the air unless otherwise stated. Column chromatography was carried out with nonactivated alumina, 80−200 mesh or silica gel, particle size finer than 230 mesh; the column size was typically 32 × 5.5 cm for alumina and 27 × 7.5 for silica gel. $[Cu(TMPA)Cl](PF_6)$ was synthesized by the literature procedure.[20−22]

Synthesis of Ligands. Methyl(6-bromomethyl)nicotinate, TMPAE, TMPAOH, and TMPACl (see Scheme 1) were synthesized as previously described.[2,23,24]

DO. TMPACl (0.98 g, 2.9 mmol) and lithium aluminum hydride (0.61 g, 25 mmol) were transferred to a 100 mL Schlenk flask and cooled to 4 °C in an ice bath. A solution of TMPAOH (0.92 g, 2.9 mmol) in 40 mL of freshly distilled THF was degassed and added

(5) Karlin, K. D.; Kaderli, S.; Zuberbühler, A. D. *Acc. Chem. Res.* **1997**, *30*, 139−147.
(6) Mirica, L. M.; Ottenwaelder, X.; Stack, T. D. P. *Chem. Rev.* **2004**, *104*, 1013−1045.
(7) Hayashi, H.; Fujinami, S.; Nagatomo, S.; Ogo, S.; Suzuki, M.; Uehara, A.; Watanabe, Y.; Kitagawa, T. *J. Am. Chem. Soc.* **2000**, *122*, 2124−2125.
(8) Uozumi, K.; Hayashi, Y.; Suzuki, M.; Uehara, A. *Chem. Lett.* **1993**, 963−966.
(9) Schatz, M.; Becker, M.; Thaler, F.; Hampel, F.; Schindler, S.; Jacobson, R. R.; Tyeklár, Z.; Murthy, N. N.; Ghosh, P.; Chen, Q.; Zubieta, J.; Karlin, K. D. *Inorg. Chem.* **2001**, *40*, 2312−2322.
(10) Becker, M.; Heinemann, F. W.; Schindler, S. *Chem. Eur. J.* **1999**, *5*, 3124−3129.
(11) Weitzer, M.; Schindler, S.; Brehm, G.; Schneider, S.; Hoermann, E.; Jung, B.; Kaderli, S.; Zuberbuehler, A. D. *Inorg. Chem.* **2003**, *42*, 1800−1806.
(12) Wei, N.; Murthy, N. N.; Chen, Q.; Zubieta, J.; Karlin, K. D. *Inorg. Chem.* **1994**, *33*, 1953−1965.
(13) Wei, N.; Murthy, N. N.; Tyeklár, Z.; Karlin, K. D. *Inorg. Chem.* **1994**, *33*, 1177−1183.
(14) Døssing, A.; Hazell, A.; Toftlund, H. *Acta Chem. Scand.* **1996**, *50*, 95−101.
(15) Lee, D.-H.; Murthy, N. N.; Karlin, K. D. *Inorg. Chem.* **1997**, *36*, 5785−5792.
(16) Karlin, K. D.; Lee, D.-H.; Kaderli, S.; Zuberbühler, A. D. *Chem. Commun.* **1997**, 475−476.
(17) Lee, D.-H. Thesis, Johns Hopkins University, 1996.
(18) Humphreys, K. J.; Karlin, K. D.; Rokita, S. E. *J. Am Chem. Soc.* **2002**, *124*, 6009−6019.
(19) Jacobson, R. R.; Tyeklár, Z.; Karlin, K. D. *Inorg. Chim. Acta* **1991**, *181*, 111−118.
(20) Karlin, K. D.; Hayes, J. C.; Shi, J.; Hutchinson, J. P.; Zubieta, J. *Inorg. Chem.* **1982**, *21*, 4106−4108.
(21) Jacobson, R. R. Ph.D. Dissertation, State University of New York at Albany, 1989.
(22) Wei, N.; Murthy, N. N.; Karlin, K. D. *Inorg. Chem.* **1994**, *33*, 6093−6100.
(23) Lee, D.-H.; Wei, N.; Murthy, N. N.; Tyeklár, Z.; Karlin, K. D.; Kaderli, S.; Jung, B.; Zuberbühler, A. D. *J. Am. Chem. Soc.* **1995**, *117*, 12498−12513.
(24) Lucchese, B. Thesis, The Johns Hopkins University, 2003.

Scheme 1

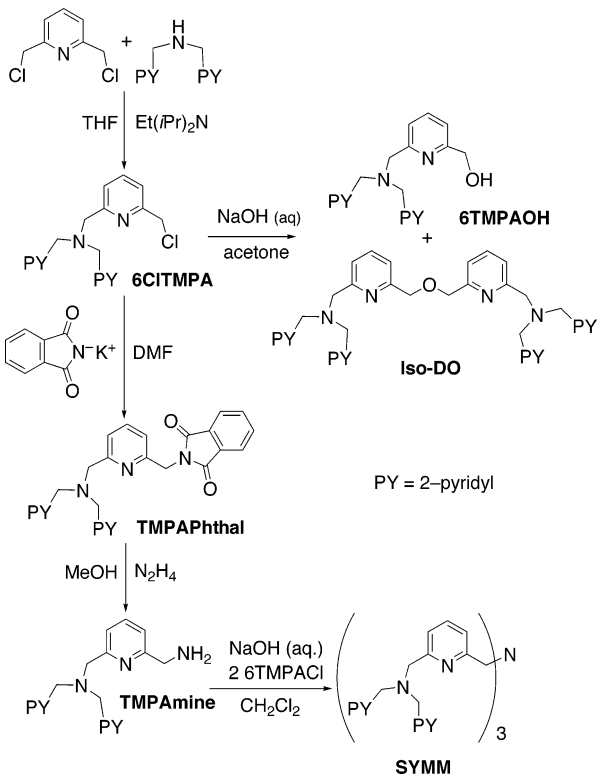

dropwise under argon to the solids. The reaction mixture was stirred under argon for 1 day at room temperature, then filtered, and concentrated under vacuum to yield a brown oil. This was redissolved in 150 mL of CH_2Cl_2, and the solution was washed three times with 150 mL of saturated Na_2CO_3. The organic layer was dried over $MgSO_4$, filtered, and concentrated by rotary evaporation to give an orange oil. The product was purified by column chromatography on alumina eluting with a gradient from 100% ethyl acetate to 3:97 methanol/ethyl acetate. Concentration of the product fractions and drying in vacuo yielded a pale yellow solid (1.1 g, yield 60%) (R_f = 0.51, alumina, 10:90 methanol/ethyl). ^{1}H NMR ($CDCl_3$): δ 3.87 (s, 12 H), 4.52 (s, 4 H), 7.10−7.13 (t, 4 H), 7.53−7.58 (t, 6 H), 7.61−7.66 (m, 6 H), 8.47−8.51 (m, 6 H). ^{13}C NMR ($CDCl_3$): δ 60.1 (CH_2), 60.3 (CH_2), 70.0 (CH_2) 123.0 (py), 123.1 (py), 131.7 (py), 136.3 (py), 136.6 (py), 148.7 (py), 149.3 (py), 159.3 (py), 159.5 (py). FAB mass spectrum: m/z 623 $(M + 1)^+$.

6ClTMPA. Bis-(2-picolyl)amine (4 g, 20.0 mmol) and 2,6-bis-(chloromethyl)pyridine (3.4 g, 19.3 mmol) were dissolved in 50 mL of distilled THF and placed in a round-bottom flask. N,N-diisopropylethylamine (20 mL, 114.8 mmol) was then added to the THF solution, and the reaction mixture was stirred at room temperature for 7 days. The pale yellow solution changed over time to an increasingly dark orange. A white powdery precipitate started to appear within the next few days. The precipitate obtained was filtered using a coarse fritted funnel and washed thoroughly with THF. The filtrate, combined with the THF solution used to wash the precipitate, was concentrated under reduced pressure to give a reddish brown oily mixture. This was dissolved in 45% ethyl acetate−55% hexanes and column chromatographed over alumina using 45% (progressively brought to 55%) ethyl acetate−55% (progressively brought to 45%) hexanes as eluent. The product fraction was collected, and the solvent was removed under reduced pressure to afford the white solid (2.6 g, 40% yield) (R_f = 0.38, alumina, 40% ethyl acetate 60% hexanes). ^{1}H NMR ($CDCl_3$): δ 3.89 (s, 6 H, 3 CH_2), 4.64 (s, 2 H, CH_2Cl), 7.14 (t, 2 H), 7.32 (d, 1 H), 7.53−7.77 (m, 6 H), 8.53 (d, 2 H).

6TMPAOH. To 6ClTMPA (1.97 g, 5.9 mmol) dissolved in 60 mL of acetone in a 250 mL round-bottom flask was added 60 mL of NaOH (1 N (aq), 60 mmol). The mixture was stirred at room temperature for 7 days. The initial pale yellow solution changed over time to orange and then to increasingly dark red. The solution neutralized with dilute HCl; at neutral pH a sudden color change from dark red to orange was noted. The solution was concentrated under reduced pressure to give a reddish brown oily mixture. This was dissolved in 3% methanol−97% dichloromethane and column chromatographed over alumina using 3% (progressively brought to 5%) methanol in dichloromethane as eluent. The product fraction was collected, and the solvent was removed under reduced pressure to afford the reddish-brown oil 6TMPAOH (0.99 g, 53% yield) (R_f = 0.30, alumina, 3% methanol−97% dichloromethane). ^{1}H NMR ($CDCl_3$): δ 3.89 (s, 6 H, 3 CH_2), 4.73 (s, 2 H, CH_2OH), 7.07 (d, 1 H), 7.16 (t, 2 H), 7.43 (d, 2 H), 7.59−7.70 (m, 5 H), 8.54 (d, 2 H). FAB mass spectrum: m/z 321 $(M + 1)^+$.

Iso-DO. To 6ClTMPA (2.0 g, 5.9 mmol) dissolved in 60 mL of acetone placed in a 250 mL round-bottom flask was added NaOH (60 mL 1 N (aq), 60 mmol). The mixture was stirred at room temperature for 7 days. The pale yellow solution changed over time to orange and then to dark red. The resulting solution was neutralized with dilute HCl, and at neutral pH a sudden color change from dark red to orange was noted. The solution was concentrated under reduced pressure to give a reddish brown oily mixture. The mixture was dissolved in 3% methanol−97% dichloromethane and column chromatographed over alumina using 3% (progressively brought to 5%) methanol in dichloromethane as eluant. The product fraction was collected, and the solvent was removed under reduced pressure to afford the off-white, solid Iso-DO (0.49 g, 27% yield) (R_f = 0.45, alumina, 3% methanol−97% dichloromethane). ^{1}H NMR ($CDCl_3$): δ 3.90 (s, 12 H, 6 CH_2), 4.73 (s, 4 H, CH_2OCH_2), 7.12 (t, 4 H), 7.36 (d, 2 H), 7.49 (d, 2 H), 7.55−7.70 (m, 10 H), 8.51 (d, 4 H). FAB mass spectrum: m/z 623 $(M + 1)^+$.

TMPAPhthal. To 6ClTMPA (0.89 g, 2.63 mmol) dissolved in 80 mL of DMF placed in a 250 mL round-bottom flask was added phthalimide, potassium derivative (0.49 g, 2.64 mmol). The reaction mixture was stirred at ≈60 °C overnight. The room-temperature cooled mixture was poured into 50 mL of deionized water, and the H_2O/DMF solution was then extracted with $CHCl_3$. The organic layer thus dehydrated by extraction with NaCl saturated aqueous solution and subsequently over Na_2SO_4 (40 min). The DMF/$CHCl_3$ solution was concentrated under reduced pressure giving an orange, oily residue which was recrystallized using diethyl ether, affording a white, needlelike crystalline product (0.88 g, 75% yield). ^{1}H NMR ($CDCl_3$): δ 3.76 (s, 2 H, 1 CH_2), 3.82 (s, 4 H, 2 CH_2) 5.00 (s, 2 H, CH_2-phthal), 7.08−7.13 (m, 3 H), 7.39 (d, 1 H), 7.51 (d, 2 H), 7.59 (t, 3 H), 7.72−7.75 (m, 2 H), 7.86−7.89 (m, 2 H) 8.49 (d, 2 H).

TMPAmine. TMPAPhthal (0.88 g, 1.96 mmol) was dissolved in 40 mL of distilled methanol placed in a 500 mL round-bottom flask, and hydrazine (0.14 g, 4.37 mmol) was added. The mixture was then stirred at 60 °C overnight and then concentrated under reduced pressure. The white, spongy residue was redissolved in $CHCl_3$, and the organic solution was extracted with 1 N NaOH and then dehydrated by extraction with NaCl saturated aqueous solution and subsequently over Na_2SO_4 (40 min). The $CHCl_3$ solution then concentrated under reduced pressure to afford the yellow/orange oily product (0.60 g, 96% yield). ^{1}H NMR ($CDCl_3$): δ 1.84 (br, 2 H, NH_2) 3.87 (s, 2 H, 1 CH_2), 3.88 (s, 4 H,

2 CH_2), 3.92 (s, 2 H, CH_2), 7.10−7.15 (m, 3 H), 7.44 (d, 1 H), 7.58−7.68 (m, 5 H), 8.52 (d, 2 H).

SYMM. TMPAmine (0.82, 2.6 mmol) and 6ClTMPA (1.74 g, 5.1) mmol were dissolved in 40 mL of dichloromethane and placed in a 500 mL round-bottom flask. To this was added 1 N NaOH (aq) (5.5 mL, 5.5 mmol) diluted with 15 mL of deionized H_2O to form a two-layered mixture. The mixture was refluxed (at the dichloromethane boiling point) for 4 days. The aqueous layer was checked for pH neutrality, and the two layers were separated. The organic layer was extracted with deionized H_2O and dehydrated through extraction with NaCl saturated aqueous solution and subsequently over Na_2SO_4 (40 min). The solution was concentrated under reduced pressure to give a reddish brown oily mixture. The mixture was dissolved in 3% methanol−97% dichloromethane and column chromatographed over alumina using 3% (progressively brought to 5%) methanol in dichloromethane as eluent. The product fraction was collected, and the solvent was removed under reduced pressure to afford the off white solid (0.93 g, 39% yield) (R_f = 0.36, alumina, 3% methanol−97% dichloromethane). ^{1}H NMR ($CDCl_3$): δ 3.84 (s, 12 H, 6 CH_2), 3.87 (s, 12 H, 6 CH_2), 7.12 (t, 6 H), 7.43 (d, 3 H), 7.48 (d, 3 H), 7.57−7.66 (m, 15 H) 8.51 (d, 6 H). FAB mass spectrum: m/z 924 $(M + 1)^+$.

Synthesis of Copper(I) Complexes. CAUTION: *Perchlorate salts of metal complexes are potentially explosive and should be handled in small quantities*. Copper(I) complexes were typically generated freshly in situ prior to each reaction by dissolving stoichiometric quantities of ligands and Cu^I salts ($Cu(CH_3CN)_4PF_6$ or $Cu(CH_3CN)_4ClO_4$ in dioxygen-free acetonitrile at room temperature under argon and in Schlenk glassware, to form bright yellow to orange to even brown colored (depending on the concentration) solutions. This procedure was utilized because of the tendency for cuprous complex disproportionation with these di- and trinucleating ligands.

$[Cu_2(DO)(CH_3CN)_2](ClO_4)_2$. Dioxygen-free CH_3CN (20 mL) was added to DO (0.312 g, 0.502 mmol) and $[Cu(CH_3CN)_4](ClO_4)$ (0.317 g, 0.853 mmol) under argon. Diethyl ether (∼60 mL) was added to the orange solution to precipitate a yellow solid. The supernatant was decanted, and the solid was recrystallized from acetonitrile/ether. The solid obtained was washed with ether and dried under vacuum (4 h), giving ∼0.4 g of orange powder (75% yield). Anal. Calcd (Found) for $C_{42}H_{44}N_{10}Cu_2O_9Cl_2$: C, 48.94 (48.77); H, 4.30 (4.36); N, 13.59 (12.43). ^{1}H NMR (d_6-acetone, 295 K): δ 2.76 (s, CH_2OCH_2), 4.96 (br, CH_2), 8.04 (br). ^{1}H NMR (d_6-acetone, 193 K): δ 3.55 (s), 3.86 (br), 4.66 (br), 7.40 (br), 7.87 (br), 8.64 (br).

$[Cu_3(SYMM)(CH_3CN)_3](PF_6)_3$. SYMM (0.1074 g, 0.116 mmol) and $Cu(CH_3CN)_4PF_6$ (0.1280 g, 0.343 mmol) were placed in a 100 mL Schlenk flask under argon. Dioxygen-free 50%−50% DMF−propionitrile mixed solvent (17 mL) was added under argon to the mixture of solids to form an orange brown solution. The Schlenk flask was placed within a dewar containing a −78 °C mixture of dry ice−acetone as 77 mL of dioxygen-free diethyl ether was added to the solution under argon in order to prompt precipitation of the complex. The flask was placed in a freezer at −80 °C. After a few days an orange brown precipitate formed. The supernatant, a still double layered (diethyl ether and propionitrile−DMF are scarcely miscible) solution, was decanted, and the residue was dried under vacuum for 1 h. ^{1}H NMR (CD_3CN, room temperature): δ 3.83, 3.96, 4.02 (br, 24 H, 12 CH_2), 7.23 (b, 6 H), 7.34 (t, 25 H), 7.79 (t, 6 H) 8.42 (br, 6 H).

$[Cu_2(Iso\text{-}DO)(CH_3CN)_2](ClO_4)_2$. Iso-DO (0.0966 g, 0.155 mmol) and $Cu(CH_3CN)_4ClO_4$ (0.1018 g, 0.311 mmol) were placed in a 50 mL Schlenk flask under argon. To the solids was added 10 mL of a dioxygen-free CH_3CN under argon and at room temperature, giving after 15−20 min of stirring an orange solution. Dioxygen-free diethyl ether (50 mL) was added to the solution to prompt precipitation of the complex. The orange-brown precipitate formed in the Schlenk flask after standing overnight in a −20 °C freezer was isolated by decantation of the supernatant and vacuum-drying. ^{1}H NMR (CD_3CN, room temperature): 3.81 (s, 8 H, 4 CH_2), 3.96 (s, 4 H, 2 CH_2), 4.83 (s, 4 H, 2 CH_2), 7.24 (s, 10 H), 7.43 (br, 2 H), 7.70 (br, 6 H) 8.37 (s, 4 H). The presence of 2 CH_3CN in the formulation was demonstrated by ^{1}H NMR spectroscopy after reduction of copper ion, as previously described.[15,24]

Synthesis of Chloro-Copper(II) Complexes. $[Cu^{II}(6TMPAOH)Cl]PF_6$; Chloroform Reaction with $[Cu(6TMPAOH)CH_3CN](PF_6)_2$. 6TMPAOH (0.0532 g, 0.166 mmol) was dissolved in 20 mL of CH_3CN, and the solution was deoxygenated by argon bubbling and then added under argon to a 50 mL Schlenk flask containing $Cu(CH_3CN)_4PF_6$ (0.0621 g, 0.167 mmol). The resulting dark yellow solution was stirred at room temperature and under argon for ∼30 min. When dioxygen-free $CHCl_3$ (3.0 mL) was added under argon, the solution ceased to look transparent, and its color instantly turned to brownish-green and then to emerald green. After ∼2 h ∼40 mL of diethyl ether was added in order to prompt precipitation of the copper complex. The precipitate was composed of a blue crystalline material and an amorphous brown residue. The blue crystalline material was recrystallized several times from CH_3CN/Et_2O. The amount of crystalline material finally isolated was 0.0456 g (49% yield). X-ray quality crystals of this compound ($[Cu(6TMPAOH)Cl]PF_6$ were obtained after precipitation, prompted by Et_2O addition to the reaction solution. Anal. Calcd for $CuC_{19}H_{20}N_4OClPF_6$: C, 40.44, H, 3.57, N, 9.93, Cl, 6.28. Found: C, 40.45, H, 3.29, N, 9.75, Cl, 6.44. UV−vis (CH_3CN): d−d bands λ_{max} nm (ϵ, M^{-1} cm^{-1}), 734 (90), 880 (100).

$[Cu^{II}_2(Iso\text{-}DO)Cl_2](PF_6)_2$. $CuCl_2 \cdot 2H_2O$ (0.028 g, 0.16 mmol) was placed in a glass vial, and 3 mL of methanol was added to the vial to form a green solution. This solution was then added to a second vial containing Iso-DO (0.050 g, 0.08 mmol). Within 30 min, all of the ligand had dissolved to form a more intensely colored solution. The resulting solution was transferred to a 50 mL round-bottom flask, diluted with 2 mL of methanol, and stirred at room temperature for about 30 min. Solid $NaPF_6$ (0.056 g, 0.33 mmol) was added to the solution, whereupon the solution became cloudy. The reaction mixture was stored in a freezer at −20 °C overnight. A light blue precipitate was collected and recrystallized from CH_3CN/Et_2O, and after vacuum-drying a dark blue crystalline material was isolated (0.0425 g, 85%). Anal. Calcd for $Cu_2C_{38}H_{38}N_8OCl_2P_2F_{12}$: C, 41.27, H, 3.45, N, 10.09. Found: C, 40.91, H, 3.25, N, 9.82. UV−vis (CH_3CN): d−d bands λ_{max} nm (ϵ, M^{-1} cm^{-1}), 726 (200), 878 (220).

$[Cu^{II}_2(Iso\text{-}DO)Cl_2](PF_6)_2$. Chloroform Reaction with $[Cu^{I}_2(Iso\text{-}DO)(CH_3CN)_2](PF_6)_2$. Iso-DO (0.0258 g, 0.041 mmol) and $Cu(CH_3CN)_4PF_6$ (0.0311 g, 0.083 mmol) were dissolved in 8 mL of dioxygen-free CH_3CN in a 25 mL Schlenk flask. The resulting dark yellow solution was stirred at room temperature under argon for ∼35 min. Dioxygen-free $CHCl_3$ (1.5 mL) was then added under argon whereupon the solution ceased to look transparent, and its color instantly turned to dark brown. After 8−10 min of stirring the solution's color started slowly to turn to green. After ∼45 min 31 mL of dioxygen-free diethyl ether was added. The precipitate formed was composed of a blue crystalline material and an amorphous brown residue. The blue crystalline material was isolated by recrystallization several times from CH_3CN/Et_2O. The amount of crystalline material finally isolated was 0.0258 g (54% yield). X-ray quality crystals of this compound ($[Cu_2Cl_2(Iso\text{-}DO)](PF_6)_2$

were obtained after precipitation, prompted by Et_2O, from the reaction solution. UV−vis (CH_3CN): d−d bands λ_{max} nm (ϵ, M^{-1} cm^{-1}), 726 (200), 878 (220). FAB mass spectrum: *m*/*z* 965.0 $(M^{2+} + (PF_6)^-)^+$.

$[Cu_3(SYMM)Cl_3](PF_6)_3$. $CuCl_2 \cdot 2H_2O$ (0.029 g, 0.170 mmol) was placed in a glass vial, and methanol (3 mL) was added to form a green solution. This solution then added to a second vial containing SYMM (0.050 g, 0.054 mmol). Within 30 min all of the ligand had dissolved to form an intensely blue colored solution. This was transferred to a 50 mL round-bottom flask, diluted with 5 mL of methanol, and stirred at room temperature for about 30 min, whereupon solid $NaPF_6$ (0.059 g, 0.351 mmol) was added. A light blue cloudiness appeared immediately upon addition. The mixture was stored in a freezer at −20 °C overnight, and the resulting light blue precipitate was collected and recrystallized from CH_3CN/Et_2O. After vacuum-drying, the dark blue crystalline material weighed 0.0566 g (65%). Anal. Calcd for $Cu_3C_{57}H_{57}N_{13}Cl_3P_3F_{18}$: C, 41.34, H, 3.47, N, 10.99. Found: C, 41.43, H, 3.44, N, 10.80. UV−vis (CH_3CN): d−d bands λ_{max} nm (ϵ, M^{-1} cm^{-1}), 738 (250), 878 (220).

$[Cu^{II}_3(SYMM)Cl_3](PF_6)_3$. $CHCl_3$ Reaction with $[Cu^{I}_3(SYMM)(CH_3CN)_3](PF_6)_3$. SYMM (0.0510 g, 0.055 mmol) and $Cu(CH_3CN)_4PF_6$ (0.0610 g, 0.164 mmol) were dissolved in 10 mL of dioxygen-free CH_3CN in a 25 mL Schlenk flask. Dioxygen-free $CHCl_3$ (3 mL) was added to the resulting dark yellow solution after 25 min under argon and at room temperature. The solution ceased to look transparent, and its color instantly turned to dark brown. After ≈20 min, the solution's appearance turned to transparent and its color to emerald green. Dioxygen-free ethyl ether (95 mL) was added, and the precipitate obtained was composed of a green homogeneous material and an amorphous brown residue. The green material was isolated by recrystallization several times from CH_3CN/Et_2O to finally give a blue crystalline material weighing 0.0380 g (41% yield). X-ray quality crystals of this compound ($[Cu_3(SYMM)Cl_3](PF_6)_3$ were obtained after recrystallization from CH_3CN/Et_2O. d−d bands λ_{max} nm (ϵ, M^{-1} cm^{-1}), 738 (250), 878 (220).

$[Cu^{II}_2(DO)Cl_2](PF_6)_2$. $CuCl_2 \cdot 2H_2O$ (0.12 g, 0.70 mmol) was placed in a glass vial, and methanol (3 mL) was added forming a green solution. This solution was then added to a second vial containing DO (0.2 g, 0.32 mmol). Within 30 min, all of the ligand had dissolved to form a more intensely colored green solution, which was transferred to a 50 mL round-bottom flask and diluted with 2 mL of methanol. The solution was stirred at room temperature for 30 min, and solid $NaPF_6$ (0.256 g, 1.52 mmol) was added. A light green cloudiness appeared immediately upon addition, and the mixture was stored in a freezer at −20 °C overnight. The resulting greenish-blue precipitate was collected and recrystallized from CH_3CN/Et_2O, and after vacuum-drying a light greenish-blue crystalline material was isolated weighing 0.267 g (72%). Anal. Calcd for $Cu_2C_{40}H_{41}N_9OCl_2P_2F_{12}$: C, 41.71, H, 3.59, N 10.94, Cl, 6.16. Found: C, 41.79, H, 3.40, N, 10.99, Cl, 6.37. UV−vis (CH_3CN): d−d bands λ_{max} nm (ϵ, M^{-1} cm^{-1}), 738 (130), 940 (320).

$[Cu^{II}_2(DO)Cl_2](PF_6)_2$. Chloroform Reaction with $[Cu^{I}_2(DO)(CH_3CN)_2](PF_6)_2$. DO (0.0507 g, 0.081 mmol) and $Cu(CH_3CN)_4PF_6$ (0.0621 g, 0.167) mmol were dissolved in 10 mL of dioxygen-free CH_3CN in a 50 mL Schlenk flask under argon. To the resulting dark yellow solution under argon was added dioxygen-free $CHCl_3$ (3 mL). Upon addition the solution color almost instantly turned to green. After 30 more minutes 30 mL of dioxygen-free ethyl ether was added. In the next few days a green crystalline precipitate formed (0.0555 g, 58% yield). X-ray quality crystals of this compound ($[Cu_2(DO)Cl_2](PF_6)_2$ were obtained after recrystallization from CH_3CN/Et_2O. Anal. Calcd for $Cu_2C_{41}H_{42.5}N_{9.5}OCl_2P_2F_{12}$: C, 42.01, H, 3.65, N 11.35, Cl, 6.05. Found: C, 42.12, H, 3.42, N, 11.19, Cl, 6.56. UV−vis (CH_3CN): d−d bands λ_{max} nm (ϵ, M^{-1} cm^{-1}), 738 (130), 940 (320).

^{2}H NMR of $CDCl_3$ Degradation Products. Iso-DO (0.0396 g, 0.064 mmol) and $Cu(CH_3CN)_4PF_6$ (0.0461 g, 0.124 mmol) were placed in a 25 mL flask under argon. The Schlenk flask then placed into the glovebox and to the mixture of solids was added degassed acetonitrile (5 mL). The mixture was then stirred at room temperature for 10−15 min leading to formation of a clear yellow-orange solution. To this solution were then added 10 μL (0.125 mmol) of degassed $CDCl_3$ (density = 1.5). The Schlenk flask was immediately capped as the solution color immediately turned to brown, becoming increasingly dark over the next several minutes. Within 35−40 min of stirring, the solution's color turned to emerald green. After about 7 h total, the reaction mixture was transferred to an NMR tube, and its cap was 'sealed' with Parafilm before removal from the glovebox. A second similarly 'sealed' NMR sample was prepared in the glovebox from a stirred solution of 10 μL of $CDCl_3$ added to 5 mL of CH_3CN in a glass vial. ^{2}H NMR spectra of the two samples were obtained: Reaction mixture, ^{2}H NMR (CH_3CN): δ 1.9 (CDH_2CN, natural abundance), 2.5, ∼3.5, 5.5, ∼5.8, 7.6, 9.2; $CDCl_3$ in CH_3CN, δ 7.6. The ratio between the integral of the $CDCl_3$ peak and the sum of all others (except CDH_2CN) was ∼1:0.7.

3,3′,5,5′-Tetra-*tert*-butyl-2,2′-dihydroxybiphenyl. In the glovebox, $[Cu_2(Iso\text{-}DO)(CH_3CN)_2](ClO_4)_2$ (0.077 g, 0.075 mmol) and 2,4-di-*tert*-butylphenol (0.100 g, 0.485 mmol) were placed in a 25 mL Schlenk flask. The mixture of solids was then dissolved in 5 mL of dioxygen-free CH_3CN. The resulting yellow-orange solution was then stirred for a few minutes, and dioxygen-free $CDCl_3$ (11.5 μL, 0.144 mmol) was added. The Schlenk flask was then immediately recapped, and the solution was stirred vigorously. Almost immediately the solution's color turned brown, and it grew darker over the next few minutes. The mixture was then stirred for the next 5−6 h, but after 1.5−2 h the solution was emerald green and transparent. A sample of the reaction mixture was transferred (in the drybox) to an NMR tube which was 'sealed' with Parafilm prior to removal from the glovebox. The ^{2}H NMR spectrum of this sample showed peaks at δ 1.9 (CDH_2CN natural abundance), 2.5, 3.5, 4.2, 5.6, 5.8, 5.9, 6.6, 7.6 ($CDCl_3$), and 9.2. The ratio between the integral of the $CDCl_3$ peak and the sum of those of all the others (except CDH_2CN) was ≈1:1. The Schlenk flask containing the rest of the reaction mixture was taken out of the drybox, and an excess of diethyl ether was added to the CH_3CN solution to cause precipitation of the copper complex. After being placed overnight in a −20 °C freezer, a solid green precipitate was visible on the bottom of the flask, while the supernatant solution was colorless. The mixture was filtered through a coarse fritted funnel, and the solvent was removed by rotary evaporation. The yellow, oily residue, which separated as a crystalline material over time, weighed 0.089 g (89% recovery) and contained a mixture of (only) 2,4-di-*tert*-butylphenol and 3,3′,5,5′-tetra-*tert*-butyl-2,2′-dihydroxybiphenyl in a ratio 1:0.156 (by ^{1}H NMR spectroscopy), implying a yield of diphenol from the monophenol derivative of 85% per copper center. (R_f = 0.32, silica, hexanes). ^{1}H NMR ($CDCl_3$): δ 1.31 (s, 18 H, 6 CH_3), 1.44 (s, 18 H, 6 CH_3), 5.22 (s, 2 H, 2 OH), 7.10 (d, 2 H), 7.38 (d, 2 H). FAB mass spectrum: *m*/*z* 410 M^+.

Control Experiment for the Formation of 3,3′,5,5′-Tetra-*tert*-butyl-2,2′-dihydroxybiphenyl. In the glovebox, using a flame-dried 10 mL Schlenk flask, dioxygen-free acetonitrile (1.5 mL) was added to a mixture of $[Cu_2Cl_2(Iso\text{-}DO)](PF_6)_2$ (0.0237 g, 0.021 mmol) and 2,4-di-*tert*-butylphenol (0.0329 g, 0.159 mmol). To the resulting

clear, dark blue solution was then added 3 μL of dioxygen-free $CDCl_3$ (0.037 mmol), and the mixture was stirred at room temperature for 6 h. The Schlenk flask was taken out of the glovebox, and the contents were extracted with *n*-pentane. The *n*-pentane layer was freed of solvent under reduced pressure to yield a solid whitish residue (0.0217 g; 66%), identified by ^{1}H NMR spectroscopy as unreacted 2,4-di-*tert*-butylphenol. To the remaining blue colored acetonitrile solution was added an excess of diethyl ether, and the solution was kept at −20 °C overnight. A blue solid separated the next day from a now colorless supernatant solution. The mixture was filtered through a coarse fritted funnel, and the filtrate was freed of solvent under reduced pressure. The oily yellowish residue product (0.0086 g, 26%) was also identified (^{1}H NMR spectroscopy) as composed of *only* intact 2,4-di-*tert*-butylphenol.

Electrochemistry. Cyclic voltammetry was carried out with a Bioanalytical Systems BAS-100B electrochemistry analyzer connected to a HP-7440A plotter. The cell was a three-neck 10 mL round-bottom flask. A glassy carbon electrode was used as the working electrode, whereas a platinum wire was used as the auxiliary electrode. The reference electrode used was S.C.E, but potentials were referenced to the ferrocinium/ferrocene couple. The measurements were performed at room temperature in a 0.1 M solution of tetrabutylammonium hexafluorophosphate ($TBAPF_6$) in DMF containing 10^{-3}−10^{-4} M of the copper complex. Solutions were deoxygenated by thorough bubbling with Ar (∼15 min). The scan rate for all profiles was 100 mV/s.

Results and Discussion

New Ligands. A series of new TMPA-based ligands has been synthesized (Chart 1), and developing chemistry is described here, in particular the reactions of copper(I) complexes with $CHCl_3$ and the detailed characterization of chloro-copper(II) products. The ligands are all characterized by the fact that one of the pyridyl rings of TMPA bears a 6′ (i.e., ortho) substituent. The binucleating Iso-DO ligand has been designed in order to explore further structure/reactivity relationships that binuclear TMPA-based systems display in their interaction with dioxygen or other substrates (i.e., organohalides; see below) of interest. The trinucleating ligand, SYMM, has also been developed in order to widen further the scope of this probe to include potential models for the T2/T3 trinuclear active site of blue copper oxidases.[25,26] The chemistry of the cuprous complexes of a mononuclear ligand, which is the precursor in the synthesis of Iso-DO, 6TMPAOH (Chart 1), has also been explored.

Synthetic procedures for these ligands are outlined in Scheme 1, and details are provided in the Experimental Section.

Reductive dechlorination experiments were also conducted on a cuprous complex based on the binucleating ligand, DO, previously developed and its Cu-dioxygen reactivity studied.[15,16] DO is an isomer of Iso-DO in which the ether linkage, which joins together the two TMPA moieties which make up the ligand, connects 5′ (or meta) pyridyl positions as opposed to the 6′ (or ortho) positions of Iso-DO (Chart 1). The synthesis of the ligand and dicopper(I) complex has not been previously reported. DO was synthesized through a multistep process summarized in Scheme 2 proceeding via improved versions of the procedures utilized previously to synthesize the intermediates methyl 6-(bromomethyl)nicotinate,[2] TMPAE,[2] TMPAOH,[23] and TMPACl.[23]

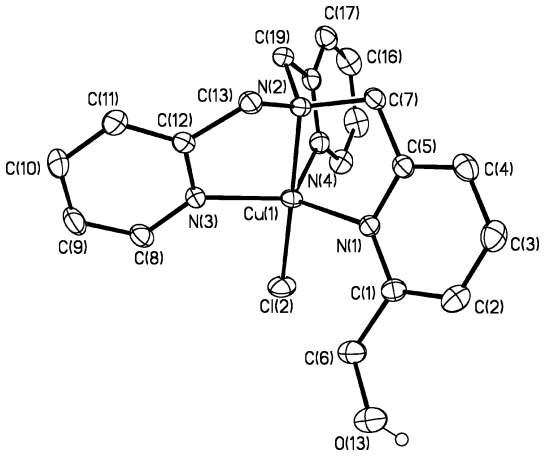

Figure 1. Cationic portion of the crystal structure of [Cu(6TMPAOH)-Cl]PF_6 (**1**). Selected bond lengths (Å) and angles (deg): Cu(1)−Cl(2): 2.2360(10), Cu(1)−N(1): 2.185(3), Cu(1)−N(2): 2.028(3), Cu(1)−N(3): 2.076(3), Cu(1)−N(4): 2.050(4). N(2)−Cu(1)−Cl(2): 174.37(10), N(3)−Cu(1)−N(4): 126.10(13), N(1)−Cu(1)−N(3): 107.47(13), N(1)−Cu(1)−N(4): 118.66(13).

Scheme 2

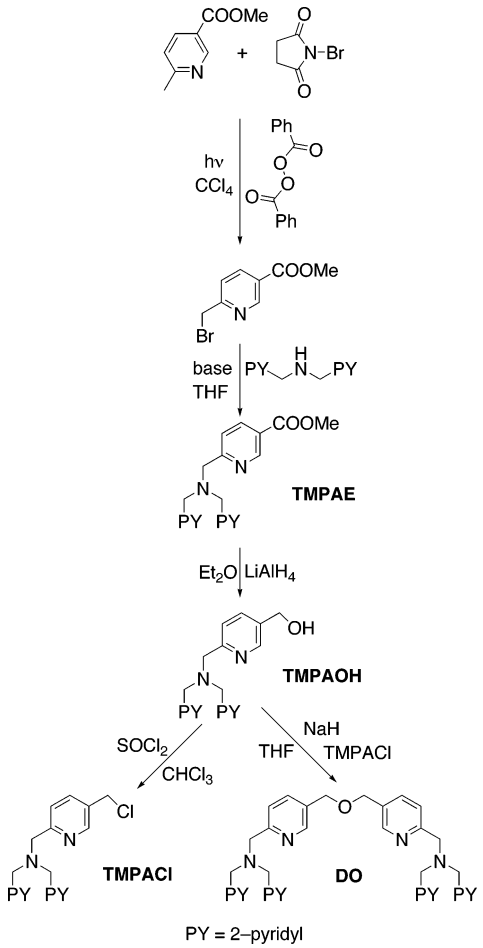

(25) Solomon, E. I.; Sundaram, U. M.; Machonkin, T. E. *Chem. Rev.* **1996**, *96*, 2563−2605.
(26) Solomon, E. I.; Chen, P.; Metz, M.; Lee, S.-K.; Palmer, A. E. *Angew. Chem., Int. Ed. Engl.* **2001**, *40*, 4570−4590.

Copper(I) Complexes. Cuprous complexes of all ligands were prepared by dissolving stoichiometric amounts of ligands and cuprous salts $Cu(CH_3CN)_4PF_6$ or $Cu(CH_3CN)_4ClO_4$ in CH_3CN. Copper(I) complex precipitates with 6TMPAOH, DO, Iso-DO, and SYMM ligands were obtained by utilizing diethyl ether as cosolvent (see Experimental Section). As seen before,[2,12,27] copper(I) complexes with TMPA-like ligands are reasonably stable and can be handled in nitrile solvents; the complexes isolated were assumed (but not entirely proven) to possess one coordinated CH_3CN molecule per tetradentate ligand−copper moiety, as has been proven for the parent mononuclear complex $[Cu^I(TMPA)(CH_3CN)]^+$,[2] $[Cu^I(TMPAE)(CH_3CN)]^+$ (TMPAE, see Scheme 2),[2] and others.[23] However, the solutions and even the solids tend to be unstable to oxidation even in the absence of dioxygen, most likely by way of disproportionation to copper metal and copper(II). While quite reassuring CD_3CN ^1H NMR spectra of redissolved solids were obtained for the precipitated and isolated diamagnetic Cu^I complexes of SYMM and Iso-DO (see Experimental Section), in most cases the reduced solutions of all ligand−copper(I) complexes were prepared in situ and then utilized immediately for reactivity studies.

Chloroform Dechlorination. Yellow colored reduced copper complexes of 6TMPAOH, DO, Iso-DO, and SYMM prepared in situ in CH_3CN, utilizing $Cu(CH_3CN)_4PF_6$ as the Cu^I source, react almost instantly at room temperature with $CHCl_3$ in the absence of O_2 to form first an intensely brown colored opaque solution which turns transparent and emerald green in color over the next ∼15 min. Precipitation of the resulting copper(II) salts with diethyl ether yielded green to blue crystalline materials obtained in good but not high yields, which were identified (a) by way of X-ray crystallography, (b) by comparison of UV features of independently synthesized complexes, and (c) mass spectrometry and/or elemental analysis on compounds formulated as $[Cu^{II}_x(L)Cl_x](PF_6)_x$.

Crystal Structures of Chloro-Copper(II) Complexes $[Cu(6TMPAOH)Cl]PF_6$ (1), $[Cu_2(DO)Cl_2](PF6)_2\cdot 2CH_3CN$ (2), $[Cu_2(Iso\text{-}DO)Cl_2](PF_6)_2\cdot CH_3CN$ (3), and $[Cu_3(SYMM)Cl_3](PF_6)_3\cdot CH_3CN$ (4). X-ray crystal structures of the chlorinated complexes as isolated from the reaction mixture in which cuprous complexes oxidation had been effected in the presence of chloroform are reported in Figures 1−4. All copper(II) ions are five-coordinate, possessing four nitrogen ligands (three pyridyl and one tertiary alkylamino nitrogen) supplied by the chelating ligands. The fifth ligand is a chloride ion covalently bound to the Cu^{II} center and most assuredly supplied from $CHCl_3$, by way of its reductive dechlorination. Some further evidence for this supposition is given below.

The structure of $[Cu_2(DO)Cl_2](PF_6)_2\cdot 2CH_3CN$ (**2**) (Figure 2) possesses an inversion center (at the ether oxygen of the ligand), thus the copper ion centers are equivalent. The structures of the other two polynuclear complexes ($[Cu_2(Iso\text{-}DO)Cl_2](PF_6)_2\cdot CH_3CN$ (**3**) and $[Cu_3(SYMM)Cl_3](PF_6)_3\cdot CH_3CN$ (**4**)) instead display no such feature, with every copper coordination site within the complex differing from the other(s). Also, in $[Cu_2(DO)Cl_2](PF_6)_2\cdot 2CH_3CN$ (**2**), the copper ion moieties are quite extended away from each other in the solid, Cu(1)···Cu(1a) = 12.2 Å (Figure 2). In $[Cu_2(Iso\text{-}DO)Cl_2](PF_6)_2\cdot CH_3CN$ (**3**) and $[Cu_3(SYMM)Cl_3](PF_6)_3\cdot CH_3CN$ (**4**), the cupric centers appear to be far enough to be noninteracting and reasonably independent of one another (see also below the EPR discussion), but they are much closer in the solid state, Cu(1)···Cu(2) = 6.6 Å in **3** while Cu(1)···Cu(2) = 8.0 Å, Cu(1)···Cu(3) = 8.0 Å and Cu(2)···Cu(3) = 6.2 Å in **4** (Figures 3 and 4).

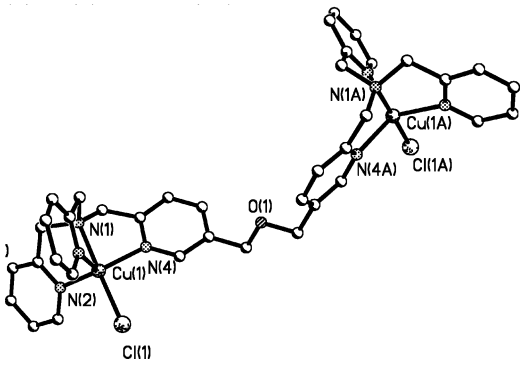

Figure 2. Cationic portion of the crystal structure of $[Cu_2(DO)Cl_2](PF_6)_2\cdot 2CH_3CN$ (**2**). Selected bond lengths (Å) and angles (deg): Cu(1)−Cl(1): 2.2296(12), Cu(1)−N(1): 2.032(4), Cu(1)−N(2): 2.059(5), Cu(1)−N(3): 2.089(4), Cu(1)−N(4): 2.054(4). N(1)−Cu(1)−Cl(1): 178.22(14), N(2)−Cu(1)−N(3): 115.84(16), N(4)−Cu(1)−N(2): 122.58(17), N(4)−Cu(1)−N(3): 114.61(16). Cu(1)···Cu(1a): 12.2 Å.

Table 1. **A**−**R** Derived τ Values for the $[Cu_x^{II}(L)Cl_x]^{x+}$ Complex Series

complex	τ
1	0.80
2	1.04 (Cu_1,Cu_{1a})
3	0.88 (Cu_1)
	0.72 (Cu_2)
4	0.17 (Cu_1)
	0.82 (Cu_2)
	0.63 (Cu_3)

The Addison-Reedijk geometry analysis[28] (**A**−**R**) allows for the semiquantitative estimation of the prevalent geometry, square pyramidal (*SP*) versus trigonal bipyramidal (*TBP*), in five-coordinate metal complexes. In this approach a parameter τ is introduced, which is an index of the degree of trigonality of the structure, calculated using observed L−M−L′ basal angles. Within the structural continuum between trigonal bipyramidal and square pyramidal limiting geometries in five-coordinate systems, τ is equal to zero for a perfect square pyramidal geometry, and one for the perfect trigonal bipyramidal. By applying the **A**−**R** method to the structures of these chlorinated complexes (see Table 1), values are obtained that indicate that, at least in crystalline phase, $[Cu_2(DO)Cl_2](PF_6)_2$ (**2**) displays an almost ideal *TBP* geometry, whereas the other three systems have a substantial, if not prevalent, *SP* geometry. These structural preferences appear to be retained in solution, see EPR spectroscopy discussion, below.

(27) Karlin, K. D.; Wei, N.; Jung, B.; Kaderli, S.; Niklaus, P.; Zuberbühler, A. D. *J. Am. Chem. Soc.* **1993**, *115*, 9506−9514.

(28) Addison, A. W.; Rao, T. N.; Reedijk, J.; van Rijn, J.; Verschoor, G. C. *J. Chem. Soc., Dalton Trans.* **1984**, 1349−1356.

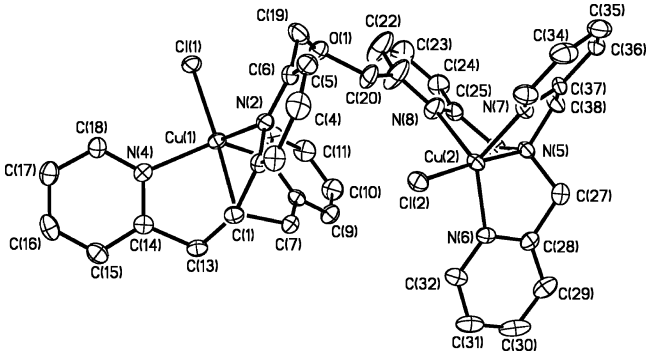

Figure 3. Cationic portion of the crystal structure of $[Cu_2(Iso\text{-}DO)Cl_2](PF_6)_2 \cdot CH_3CN$ (**3**). Selected bond lengths (Å) and angles (deg): Cu(1)−Cl(1): 2.2371(14), Cu(1)−N(1): 2.021(4), Cu(1)−N(2): 2.203(5), Cu(1)−N(3): 2.036(4), Cu(1)−N(4): 2.054(5). N(1)−Cu(1)−Cl(1): 176.85(13), N(3)−Cu(1)−N(4): 124.01(17), N(2)−Cu(1)−N(3): 105.82(18), N(2)−Cu(1)−N(4): 122.08(17). Cu(2)−Cl(2): 2.2304(14), Cu(2)−N(5): 2.032-(4), Cu(2)−N(6): 2.013(4), Cu(2)−N(7): 2.036(5), Cu(2)−N(8): 2.260(5). N(5)−Cu(2)−Cl(2): 176.74(13), N(6)−Cu(2)−N(7): 133.31(19), N(8)−Cu(2)−N(6): 119.12(19), N(8)−Cu(2)−N(7): 98.9(2). Cu(1)···Cu(2): 6.6 Å.

Within this framework, there are some further interesting or relevant points: (1) The chloride ligands in the structure of $[Cu_2(DO)Cl_2](PF_6)_2$ (**2**) are in the axial position of the trigonal-bipyramid. However, in the other structures, those all being distorted from pure *TBP* (Table 1), the chloride is either equatorial in an *SP* description, or the structure is intermediate such that one cannot necessarily define the axial ligand. (2) For distorted structure complexes **1**, **3**, and **4**, the $Cu-N_{pyridyl}$ bond length is noticeably elongated for the pyridyl moiety possessing the 6′-substituent. In comparison to Cu−N4 (or Cu−N4A) for which $Cu-N_{pyridyl} = 2.054$ (4) Å in **2**, or even the other $Cu-N_{pyridyl}$ bond lengths (2.074 ave.) in this structure, or those in $[Cu^{II}(TMPA)Cl](PF_6)$ ($Cu-N_{pyridyl} = 2.06$ to 2.07 Å), the $Cu-N_{pyridyl}$ bond lengths for the pyridyl moieties with 6′-substituents elongate by an average of 0.20 Å, with the minimum increase being 0.12 Å and the maximum being 0.40 Å. Another manifestation of the 6′- vs 5′-susbstituent deformations is the finding that, for instance in $[Cu_2(DO)Cl_2](PF_6)_2$ (**2**), the Cu(1) is only 0.16 Å out of the least-squares mean plane containing pyridyl N(4) (with 5′-substituent, Figure 2), while in $[Cu_2(Iso\text{-}DO)Cl_2](PF_6)_2$ (**3**), Cu(1) is fully 0.95 Å out of the plane containing pyridyl N(4) (Figure 3). These distortions are thus significant and most likely occur due to steric effects of the pyridyl 6′-substituent in **1**, **3**, and **4** becoming too close to the copper(II) ion and/or the chloride ligand. Such steric effects and bond length elongations have also been seen in substituted-TMPA iron complex structures described by Que and co-workers.[29,30] Obviously, such interactions are not present or possible with the 5′-substituents in $[Cu_2(DO)Cl_2](PF_6)_2 \cdot 2CH_3CN$ (**2**).

Electrochemistry. Half-wave potentials ($E_{1/2}$) of all of the copper(II) complexes were measured at room temperature in dioxygen-free dimethylformamide (DMF) using cyclic voltammetry. As can be seen from Table 2, the voltammograms complexes **1**−**3** are indicative of (quasi) reversible redox processes.

Table 2. Reduction Potentials[a] of Complexes $[Cu_x^{II}(L)Cl_x]^{x+}$ in DMF at Room Temperature

L	E_{pc}	E_{pa}	$E_{1/2}$	i_{pa}/i_{pc}
TMPA	−0.85	−0.77	−0.81	0.85
6TMPAOH	−0.77	−0.67	−0.72	0.72
DO	−0.83	−0.74	−0.79	0.88
Iso-DO	−0.70	−0.63	−0.66	0.68
SYMM	−0.69			

[a] Potentials in volts, referenced to ferrocinium/ferrocene.

Tanaka and co-workers[31] already demonstrated that the introduction of a methyl substituent in the 6′ (ortho) pyridyl position in one of the pyridine rings of the TMPA ligand causes the $E_{1/2}$ of the corresponding Cu^{II} complex to shift toward more positive values. This effect is essentially cumulative and additional methyl substituents in the remaining pyridine rings shift the half-wave potential of the corresponding copper(II) complexes further to even more positive values. In particular the $E_{1/2}$ values reported for $[Cu(tpa)H_2O](ClO_4)_2$ (tpa ≡ TMPA) in CH_3CN is −0.42 V, and this shifts to −0.33 V when the ligand is Me_1−tpa (TMPA carrying one 6′-pyridyl methyl substituent), to −0.20 when it is Me_2−tpa (carrying two 6′-pyridyl methyl substituents), and to −0.04 for the copper(II) complex with Me_3−tpa. The progressive 'addition' of 6′-pyridyl methyl substituents also increases the separation between the reduction and oxidation peaks in the cyclic voltammetry profile of the copper(II) complexes, indicative of a less reversible behavior of the electron-transfer process at the electrode surface.

As can be seen from Table 2, similar effects are encountered for our series of $[Cu_x^{II}(L)Cl_x]^{x+}$ complexes. Two 6′-pyridyl substituted complexes $[Cu(6TMPAOH)Cl]^+$ (**1**) and $([Cu_2(Iso\text{-}DO)Cl_2]^{2+}$ (**3**) display $E_{1/2}$ values that are, respectively, ∼90 mV and ∼150 mV more positive than that observed for $[Cu(TMPA)Cl]^+$. As for the 5′-pyridyl substituted complex $[Cu_2(DO)Cl_2)]^{2+}$ (**2**), the cyclic voltammetry profile of this complex is almost indistinguishable from that of $[Cu(TMPA)Cl]^+$, Figure 5a. The $E_{1/2}$ value for this binuclear complex **2** is only ∼20 mV more positive than the corresponding value for $[Cu(TMPA)Cl]^+$, and the values for ΔEp and i_{pc}/i_{pa} are also very similar to each other (Table 2). The present data, in conjunction with evidence from closely related systems,[22,31] suggest a qualitative connection between the geometry around the copper center (square pyramidal vs trigonal bipyramidal) and the complex's reduction potential in TMPA-related systems. Pentacoordinate copper(II) complexes with nearly square pyramidal coordination geometry display more positive reduction potentials compared to those displayed by complexes in which the copper(II) center(s) find itself in a close to ideal trigonal bipyramidal coordination geometry (τ for $[Cu(TMPA)Cl]^+$: 1.01).[20,22]

The electrochemical behavior of the trinuclear complex $[Cu_3(SYMM)Cl_3]^{3+}$ (**4**) was also examined, but only ir-

(29) Zheng, H.; Dong, Y. H.; Zang, Y.; Que, L. *J. Inorg. Biochem.* **1999**, *74*, 350−350.
(30) Zang, Y.; Kim, J.; Dong, Y. H.; Wilkinson, E. C.; Appelman, E. H.; Que, L. *J. Am. Chem. Soc.* **1997**, *119*, 4197−4205.
(31) Nagao, H.; Komeda, N.; Mukaida, M.; Suzuki, M.; Tanaka, K. *Inorg. Chem.* **1996**, *35*, 6809−6815.

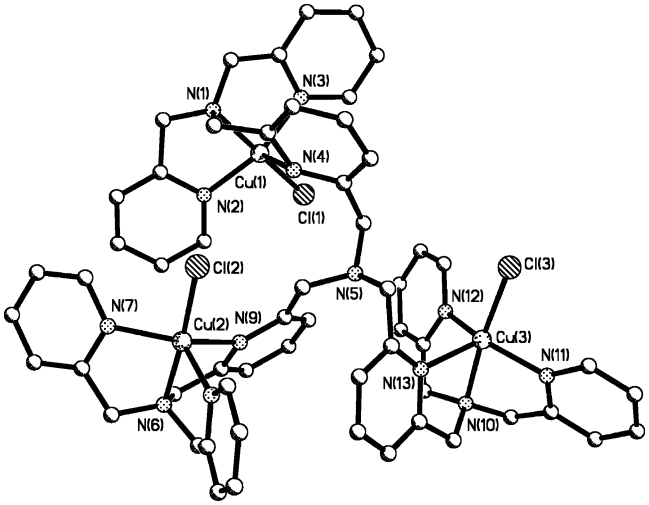

Figure 4. Cationic portion of the crystal structure of $[Cu_3(SYMM)Cl_3](PF_6)_3 \cdot CH_3CN$ (**4**). Selected bond lengths (Å) and angles (deg): Cu(1)−Cl(1): 2.257(3), Cu(1)−N(1): 2.052(9), Cu(1)−N(2): 1.936(5), Cu(1)−N(3): 1.927(5), Cu(1)−N(4): 2.467(5). N(1)−Cu(1)−Cl(1): 173.0(3), N(2)−Cu(1)−N(3): 163.0(2), N(4)−Cu(1)−N(2): 102.9(2), N(4)−Cu(1)−N(3): 81.84(19). Cu(2)−Cl(2): 2.236(3), Cu(2)−N(6): 2.004(8), Cu(2)−N(7): 1.998(7), Cu(2)−N(8): 2.061(6), Cu(2)−N(9): 2.216(5). N(6)−Cu(2)−Cl(2): 176.1(3), N(7)−Cu(2)−N(8): 126.7(3), N(9)−Cu(2)−N(7): 122.6(2), N(9)−Cu(2)−N(8): 103.1(2). Cu(3)−Cl(3): 2.242(3), Cu(3)−N(10): 2.015(8), Cu(3)−N(11): 1.979(6), Cu(3)−N(12): 2.011(5), Cu(3)−N(13): 2.201(5). N(10)−Cu(3)−Cl(3): 173.7(3), N(11)−Cu(3)−N(12): 135.7(2), N(13)−Cu(3)−N(11): 112.9(2), N(13)−Cu(3)−N(12): 103.3(2). Cu(1)···Cu(2) = 8.0 Å; Cu(1)···Cu(3) = 8.0 Å; Cu(2)···Cu(3) = 6.2 Å.

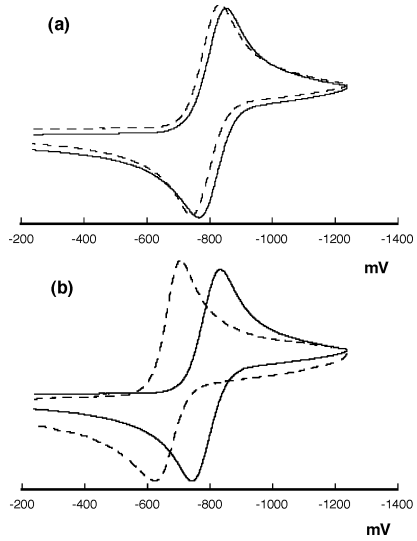

Figure 5. (a) Superposition of the cyclic voltammograms of $[Cu_2(DO)Cl_2](PF_6)_2$ (**2**) (dashed line) and [Cu(TMPA)Cl] PF_6 (solid line). (b) Superposition of the cyclic voltammograms of $[Cu_2(DO)Cl_2](PF_6)_2$ (**2**) (solid line) and $[Cu_2(Iso\text{-}DO)Cl_2](PF_6)_2$ (**3**) (dashed line). Conditions: DMF solvent, room temperature. The current values (*y* axis) are arbitrary, and concentrations vary for all voltammograms.

reversible reduction at ∼ −0.7 is observed (see Supporting Information). This observation is consistent with our finding that the in situ generated tricopper(I) complex $[Cu_3(SYMM)(CH_3CN)_3](PF_6)_3$ is quite unstable and seems to readily disproportionate. We speculate that the relatively short intramolecular Cu···Cu distances in $[Cu_3(SYMM)Cl_3]^{3+}$ (**4**) (Figure 4) may facilitate electron-transfer and thus overall disproportionation once any copper(I) site is generated.

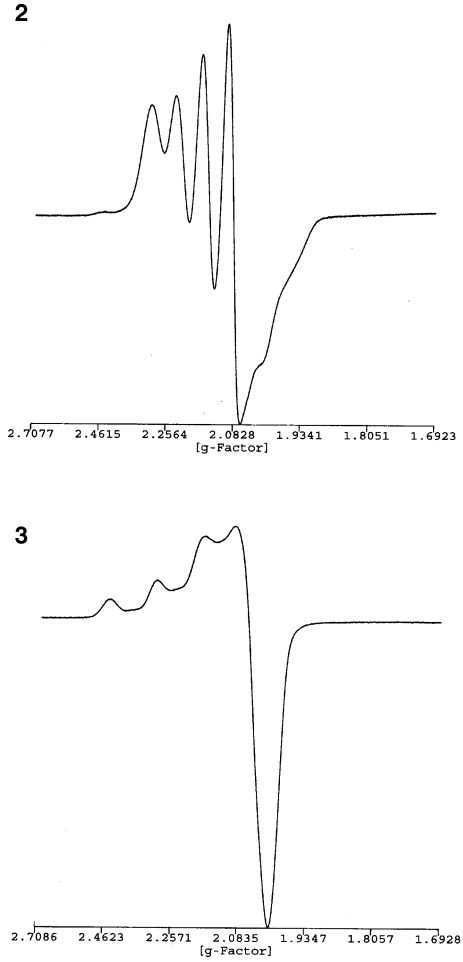

Figure 6. Reverse axial (frozen) EPR spectrum of $[Cu_2(DO)Cl_2](PF_6)_2$ (**2**) and regular axial (frozen) EPR spectrum of $[Cu_2(Iso\text{-}DO)Cl_2](PF_6)_2$ (**3**).

Table 3. EPR Spectroscopy Parameters and Hyperfine Coupling Constants A ($cm^{-1} \cdot 10^{-4}$)

complex	$g_{\|\|}$	$g_\perp$	$A_{\|\|}$	$A_\perp$
1	2.23	2.05	182	
2	2.02	2.18	80	94
3	2.20	2.02	176	
4	2.22	2.08	190	

Electron Paramagnetic Resonance (EPR). Frozen EPR spectra (T ∼ 13−16 K) of all the chloro-copper(II) complexes were obtained in DMF/toluene solvent ∼1:1 (v/v). EPR spectra and simulations of all complexes are reported in the Supporting Information. The spectrum of $[Cu_3(SYMM)Cl_3](PF_6)_3$ (**4**) is somewhat broader than the others, possibly due to weak magnetic/electronic interactions between copper(II) centers, or because of small variations in their local structure (as in fact observed in the X-ray structure, Figure 4). Frozen EPR spectra for the other complexes displayed a more than satisfactory definition. Values for these parameters are given in Table 3.

The spectra of $[Cu(6TMPAOH)Cl]PF_6$ (**1**), $[Cu_2(Iso\text{-}DO)Cl_2](PF_6)_2$ (**3**) (Figure 6, spectrum **3**), and $[Cu_3(SYMM)Cl_3](PF_6)_3$ (**4**) display EPR features typical for copper(II) ion in an axial environment, i.e., $g_{||} > 2.1 > g_\perp > 2.00$ and $A_{||} = 158-201 \cdot 10^{-4}$ cm^{-1}.[25,26,32−34] This is expected when the ground state of the copper(II) d^9 ion is $d_{x^2-y^2}$, i.e., with the unpaired copper(II) ion spin localized on a *d* orbital with a

$d_{x^2-y^2}$ symmetry. This situation is expected for a *SP* copper(II) ion geometry and generally observed for situations deviated much at all from *TBP* geometry.[22] On the other hand, the EPR spectrum of $[Cu_2(DO)Cl_2](PF_6)_2$ (**2**) (Figure 6, spectrum **2**) displays features typical of a reverse axial spectrum, i.e., $g_\perp > g_{||} \approx 2.00$ and $A_\perp \approx (60-100)10^{-4}$ cm^{-1},[32-34] expected for a copper(II) ion d_{z^2} ground state,[32-34] as expected for an ideal or barely distorted trigonal bipyramidal coordination environment. The general geometric trends encountered, as per the **A**−**R** analysis of the crystal structures of these complexes (vide supra), are retained in (frozen) solution, as indicated by the present EPR spectroscopic data. Thus, the structural differences observed in the solid state are not due to crystal packing but can be attributed to more fundamental structural requirements. The binuclear complex $[Cu_2(DO)Cl_2](PF_6)_2$ (**2**), with its 5′- and not 6′-pyridyl substituents, exhibits both crystalline and solution phase properties which closely resemble those reported (and confirmed by the present study, see Supporting Information) for the mononuclear complex $[Cu(TMPA)Cl]^+$ (τ (**A**−**R** analysis) = 1.01,[20,22] $g_\perp = 2.18$[22] $g_{||} = 2.01$, $A_\perp = 96 \times 10^{-4}$ cm^{-1}). The presence of a substituent in the 5′-pyridyl position of the 'linker' in **2** has little or no effect on the coordination geometry around the copper centers. The two connected copper-TMPA moieties, in fact, behave essentially like two independent $[Cu(TMPA)Cl]^+$ cations. The lack of any significant electronic interaction (through space or through bond) between the Cu ions is also made evident by the unbroadened, 'normal' nature of the EPR spectrum.[35,36]

Copper(I) Complex Mediated Dehalogenation. Detoxification or, more generally, remediation of halogenated (particularly chlorinated) organic R−X pollutants, has been the focus of much attention.[37,38] Thus, there is some interest in the reactions described here, wherein copper(I) complexes with the TMPA-like ligands effect organohalide (i.e., chloroform) reductive dehalogentation reactions. In fact, this follows previous observations[2] that $[Cu^I(TMPA)CH_3CN]PF_6$ was unstable at room temperature in dichloromethane, undergoing oxidation in the absence of dioxygen, due to dechlorination of the solvent and formation of a Cu^{II}−Cl covalent bond. That finding was followed up with a more general study, showing that $[Cu^I(TMPA)CH_3CN]PF_6$ could be used as a reductive coupling agent for benzyl and allyl halides:[19]

$$ArCH_2X + [Cu^I(TMPA)CH_3CN]PF_6 \rightarrow 1/2ArCH_2CH_2Ar + [Cu^{II}(TMPA)X]PF_6$$

A few other ligand−copper(I) complexes are also known to effect reductive dehalogenation reactions.[12,13,19,22,23,39-46] Copper enzymes such as such as the dopamine β-monooxygenase[47,48] and ammonia monooxygenase[49-54] also effect both reductive and oxidative transformations of halocarbons substrates, depending on their oxidation state and presence of dioxygen. The 'blue' multicopper oxidase fungal laccase has recently been shown to be able to dehalogenate chlorinated hydroxybiphenyls.[55]

Chloroform Dehalogenation. Thus, it was of interest to obtain further insights into the dehalogenation reactions carried out with the copper(I) complexes of 6TMPAOH, DO, Iso-DO, and SYMM. In these early studies as part of a broader program, chloroform was chosen as a substrate. A deuterium ^2H NMR experiment was devised in order to confirm that indeed the formation of a Cu^{II}−Cl bond from a solution of a copper(I) complex occurred concomitantly with chloroform degradation.

A stoichiometric amount of deuterated chloroform ($CDCl_3$, one equiv per copper center) was reacted with $[Cu^I_2(Iso\text{-}DO)(CH_3CN)_2](PF_6)_2$, see Experimental Section. Following workup, a ^2H NMR spectrum of the reaction mixture was compared with that of the same amount of pure $CDCl_3$ in CH_3CN (Figure 7). The reference spectrum (**a**) shows only peaks due $CDCl_3$ (7.56 ppm) and natural abundance CDH_2-CN (1.94 ppm). But the spectrum of the reaction mixture (**b**) displays 'extra' peaks at ~2.5, 3.3, 5.5, 5.8, and 9.2 ppm. As the only reasonable source of deuterium in the reaction mixture is the $CDCl_3$ added, the compounds associated with these new peaks must be derived from this substrate and its reaction degradation products. Dichloromethane (as $CDHCl_2$ (5.5 ppm)) is an expected[56] reduction product and formal-

(32) Barbucci, R.; Bencini, A.; Gatteschi, D. *Inorg. Chem.* **1977**, *16*, 2117−2220.
(33) Senyukova, G. A.; Mikheikin, I. D.; Zamaraev, K. I. *J. Struct. Chem.* **1970**, *11*, 18−21.
(34) Jiang, F.; Karlin, K. D.; Peisach, J. *Inorg. Chem.* **1993**, *32*, 2576−2582.
(35) Smith, T. D.; Pilbrow, J. R. *Coord. Chem. Rev.* **1974**, *13*, 173−278.
(36) Smith, T. D.; Martell, A. E. *J. Am. Chem. Soc.* **1972**, *94*, 4123−29.
(37) Castro, C. E. *Rev. Environ. Contam. Toxicol.* **1998**, *155*, 1−67.
(38) Wackett, L. P.; Schanke, C. A. *Met. Ions Biol. Syst.* **1992**, *28*, 329−356.
(39) Lipshutz, B. H.; Parker, D.; Kozlowski, J. A.; Miller, R. D. *J. Org. Chem.* **1983**, *48*, 3334−3336.
(40) Mochida, I.; Noguchi, H.; Fujitsu, H.; Seiyama, T.; Takeshita, K. *Can. J. Chem.* **1977**, *55*, 2420−2421.
(41) Nondek, L.; Hun, L. G.; Wichterlova, B.; Krupicka, S. *J. Mol. Catal.* **1987**, *42*, 51−55.
(42) Hájek, M.; Silhavy, P.; Malek, J. *Collect. Czech. Chem. Commun.* **1980**, *45*, 3502−3509.
(43) Hájek, M.; Silhavy, P. *Collect. Czech. Chem. Commun.* **1983**, *48*, 1710−1717.
(44) Kern, J.-M.; Sauvage, J.-P. *J. Chem. Soc., Chem. Commun.* **1987**, 546−548.
(45) Yanada, R.; Akiyama, T.; Harayama, T.; Yanada, K.; Meguri, H.; Yoneda, F. *J. Chem. Soc., Chem. Commun.* **1989**, 238−239.
(46) Nasir, M. S.; Cohen, B. I.; Karlin, K. D. *Inorg. Chim. Acta* **1990**, *176*, 185−187.
(47) Mangold, J. B.; Klinman, J. P. *J. Biol. Chem.* **1984**, *259*, 7772−7779.
(48) Colombo, G.; Rajashekhar, B.; Giedroc, D. P.; Villafranca, J. J. *Biochemistry* **1984**, *23*, 3590−3598.
(49) Arciero, D. M.; Vannelli, T.; Logan, M.; Hooper, A. B. *Biochem. Biophys. Res. Commun.* **1989**, *159*, 640−643.
(50) Vannelli, T.; Hooper, A. B. *Biochemistry* **1995**, *34*, 11743−11749.
(51) Hyman, M. R.; Wood, P. M. In *Microbial growth on C1 compound: Proceedings of the 4th International Symposium*; Crawford, R. L., Hanson, R. S., Eds.; American Society for Microbiology: Washington, DC, 1984; pp 49−52.
(52) Rasche, M. E.; Hicks, R. E.; Hyman, M. R.; Arp, D. J. *J. Bacteriol.* **1990**, *172*, 5368−5373.
(53) Vannelli, T.; Hooper, A. B. *Appl. Environ. Microbiol.* **1992**, *58*, 2321−2325.
(54) Vannelli, T.; Hooper, A. B. *Appl. Environ. Microbiol.* **1993**, *59*, 3597−3601.
(55) Schultz, A.; Jonas, U.; Hammer, E.; Schauer, F. *Appl. Environ. Microbiol.* **2001**, *67*, 4377−4381.
(56) Singh, K.; Horng, Y. C.; Ragsdale, S. W. *J. Am Chem. Soc.* **2003**, *125*, 2436−2443.

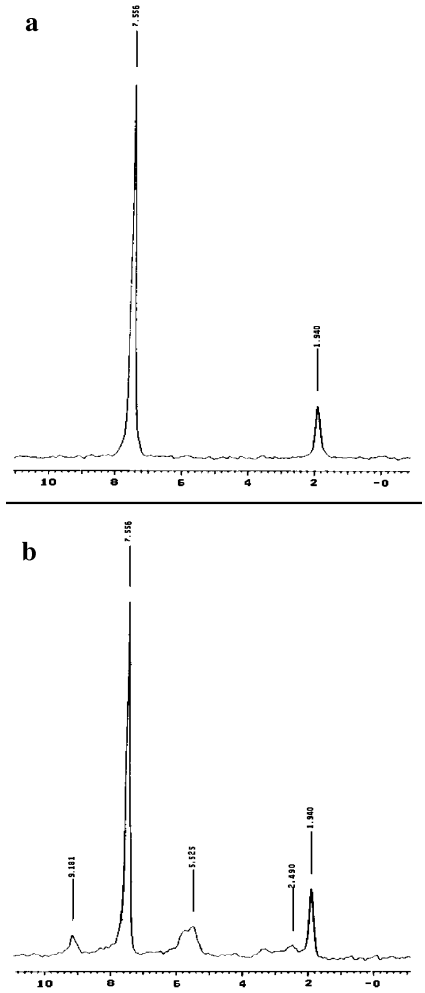

Figure 7. ^2H NMR spectra in CH_3CN of (**a**) $CDCl_3$ and (**b**) the reaction mixture following $CDCl_3$ reduction through chlorine (chloride) extraction by $[Cu_2(Iso\text{-}DO)(MeCN)_2](PF_6)_2$.

dehyde (HC(O)D, with downfield resonance ~9.2 ppm) may be present. The presence of multiple products poses unanticipated questions with regard to the course of reaction and mechanistic nuances in this copper(I) complex mediated dehalogenation. Future detailed studies are warranted.

However, one other point worth mentioning is that the presence of a sizable amount of leftover $CDCl_3$ (Figure 7**b**) ensures that chloroform must not have been the limiting reagent as the chlorine source for formation of the product $[Cu^I_2(Iso\text{-}DO)Cl_2](PF_6)_2$, which was obtained in reasonably good yield. As $CDCl_3$ was added in stoichiometric amounts, one can infer that it underwent multiple dechlorination cycles; some of the chloroform provided most or all of the chlorine which ended up on the copper product.

Radical Trapping with 2,4-Di-*tert*-butylphenol. A general mechanism of inner-sphere electron transfer for the alkyl halide oxidation of low-valent transition metal ions, such as the chromous ion, was established as early as the early 1960s.[57,58] It involves R−X coordination of the metal center followed by (the rate limiting) formation of a bond between the (oxidized) metal ion and an X^- with the concomitant release of $R^\bullet$. In an attempt to obtain some further mechanistic insights by probing for the release of free radicals in the dechlorination of $CHCl_3$ by $[Cu^I_2(Iso\text{-}DO)(CH_3CN)_2](PF_6)_2$, 2,4-di-*tert*-butylphenol (2,4(*t*Bu_2)ArOH) was employed. If $H^\bullet$ abstraction occurs, this could couple to form 3,3′,5,5′-tetra-*tert*-butyl-2,2′-dihydroxybiphenyl (see diagram).[4,59−62]

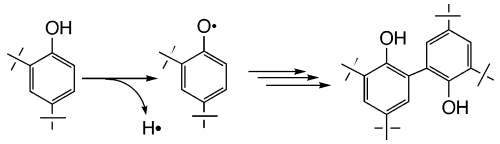

In the presence of an excess of 2,4(*t*Bu_2)ArOH, a dioxygen free CH_3CN solution of $[Cu^I_2(Iso\text{-}DO)(CH_3CN)_2](PF_6)_2$ with added one equiv $CDCl_3$ was mixed; a near stoichiometric amount (~85% per copper center) of the coupled phenol formed (see Experimental Section). In a control experiment, it was found that no reaction occurs with just $[Cu^{II}_2(Iso\text{-}DO)Cl_2]^{2+}$ mixing with excess 2,4(*t*Bu_2)ArOH. These observations thus indicate that radicals are most likely released concomitant with reductive dechlorination of chloroform. As (excess) 2,4(*t*Bu_2)ArOH is unable to reduce the product copper(II) complex $[Cu^{II}_2(Iso\text{-}DO)Cl_2](PF_6)_2$, no further reaction or catalytic turnover can occur.

A ^2H NMR spectrum of the $[Cu^{II}_2(Iso\text{-}DO)Cl_2]^{2+}/CDCl_3$/excess 2,4(*t*$Bu_2$)ArOH reaction mixture (Supporting Information, Figure S1) reveals a result similar to that described above (Figure 7). In this case, however, the product distribution and/or number of products appears qualitatively different. The observed smaller ratio for the integral of intact $CDCl_3$ compared to degradation product(s) (~1:1 versus ~1:0.7) suggests that the amount of $CDCl_3$ undergoing dechlorination may increase (relatively) in the presence of 2,4-(*t*Bu_2)ArOH. The results are hard to interpret, but we suggest that the phenol radical trap may help prevent haloalkane radical oxidation of unreacted cuprous complex species, thus enhancing the overall yield of the dehalogenation reaction.

Summary/Conclusions

All the cuprous complexes of a number of TMPA-derived ligands, mono-, di-, and trinuclear, are able to reductively dechlorinate chloroform at room temperature in acetonitrile and in the absence of dioxygen. The main inorganic product of this relatively high yield reaction is the corresponding chloro-copper(II) species, the chlorine being supplied by the $CHCl_3$ substrate. The organic product(s) of the dechlorination reaction have not been conclusively identified, although they may include CH_2Cl_2 and CH_3Cl.[56] The evidence from the stoichiometry of the reaction indicates that $CH(D)Cl_3$ may undergo multiple dechlorinations as performed by the copper-(I) complexes.

(57) Kray, W. C.; Castro, C. E. *J. Am. Chem. Soc.* **1964**, *83*, 4603−4608.
(58) Castro, C. E.; Kray, W. C. *J. Am. Chem. Soc.* **1963**, *85*, 27682−27773.
(59) Kushioka, K. *J. Org. Chem.* **1983**, *48*, 4948−50.
(60) Halfen, J. A.; Young, V. G., Jr.; Tolman, W. B. *Inorg. Chem.* **1998**, *37*, 2102−2103.
(61) Mahadevan, V.; DuBois, J. L.; Hedman, B.; Hodgson, K. O.; Stack, T. D. P. *J. Am. Chem. Soc.* **1999**, *121*, 5583−5584.
(62) Gupta, R.; Mukherjee, R. *Tetrahedron Lett.* **2000**, 7763−7767.

The dechlorination reaction mechanism is most likely radical in nature. Stoichiometric (per copper center) $H^{\bullet}$ abstraction from 2,4-di-*tert*-butylphenol is effected in the presence of the copper(I) complex of Iso-DO and $CHCl_3$. A possible mechanism for the dehalogenation is inspired by the mechanism proposed for the analogue reaction carried out by Fe^{II}−porphyrins,[63−68] as follows:

$$Cu^{I} + RX \leftrightarrow Cu^{I}(RX) \rightarrow [Cu\cdots X\cdots R] \rightarrow Cu^{II}X + R^{\bullet}$$

There is no evidence of hydrogen abstraction, when the inorganic product is $[Cu_2(\text{Iso-DO})Cl_2]^{2+}$, i.e., 2,4-di-*tert*-butylphenol is not a reductant strong enough to allow for $[Cu_2(\text{Iso-DO})Cl_2]^{2+}$ reduction to the copper(I) level. As a consequence, no catalytic turnover in chloroform dechlorination is observed. The presence of 2,4-di-*tert*-butylphenol may however render the stoichiometric dechlorination reaction more efficient possibly because the substituted phenol competes with unreacted Cu^{I} complexes for the reduction of haloalkane radicals. Further studies are necessary, with the systems studied here or others (and with substrates) more amenable to mechanistic probing.

With regard to the binuclear systems based on DO and Iso-DO, a change in the pyridyl positions acting as 'bridgeheads' for the ether group connecting the TMPA moieties (5′ versus 6′) has a significant effect on the coordination geometry around the copper centers. $[Cu_2(DO)Cl_2]^{2+}$ (**2**), with 5′ bridge-head, displays a nearly ideal trigonal bipyramidal coordination environment, while $[Cu_2(\text{Iso-DO})Cl_2]^{2+}$ (**3**) (6′-pyridyl substitution) undergoes structural distortions toward square-based pyramidal ligation in both solid (crystal) and solution phases.

Thus $[Cu_2(DO)Cl_2]^{2+}$ (**2**) displays solution and solid-state properties closely resembling the mononuclear complex $[Cu(TMPA)Cl]^{+}$, as the 5′ pyridyl linker has little or no effect on the copper ion properties. The similarity in behavior between $[Cu_2(DO)Cl_2]^{2+}$ (**2**) and $[Cu(TMPA)Cl]^{+}$ also extends to their reduction potentials, and the two copper ions in **2** act essentially independently. The distortions seen in 6′-pyridyl substituted and linked $[Cu_2(\text{Iso-DO})Cl_2](PF_6)_2$ (**3**) (as well as in $[Cu_3(SYMM)Cl_3](PF_6)_3$) result in complexes with copper(II) ions located much closer to each other in the overall binuclear (or trinuclear structure), and the half-wave reduction potential for $[Cu_2(\text{Iso-DO})Cl_2]^{2+}$ is about 150 mV more positive than that of $[Cu(TMPA)Cl]^{+}$, in accordance with trends[9,22,31] generally observed in pentacoordinate copper(II) chelates varying along the TBP versus SP geometric disposition.

Future studies will include applications of the reductive dehalogenation chemistry seen here and investigation of the effects of the ligand variations (e.g., 5′- versus 6′-pyridyl) on copper(I)-dioxygen and substrate oxidation chemistry.

Acknowledgment. We gratefully acknowledge the support of the National Institutes of Health (K.D.K., GM28962) and a National Science Foundation environmental research grant (CRAEMS, K.D.K.), as well as Chonbuk National Univ. (D.-H.L.).

Supporting Information Available: Room-temperature cyclic voltammetry profiles of **1**, **2**, **3**, **4**, and $[Cu(TMPA)Cl]^{+}$ and data (Tables 1−5), EPR spectra of chloro complexes **1**, **2**, **3**, **4**, and $[Cu(TMPA)Cl]^{+}$ and spectral simulations (Tables 6−10), and ^{2}H NMR spectrum (Figure S1) of the $[Cu(\text{Iso-DO})Cl_2]^{2+}/CDCl_3$/excess 2,4($tBu_2$)ArOH reaction mixture. This material is available free of charge via the Internet at http://pubs.acs.org.

IC0497477

(63) Wade, R. S.; Castro, C. E. *J. Am. Chem. Soc.* **1973**, *95*, 231−4.
(64) Wade, R. S.; Castro, C. E. *J. Am. Chem. Soc.* **1973**, *95*, 226−30.
(65) Castro, C. E.; Wade, R. S.; Belser, N. O. *Biochemistry* **1985**, *24*, 204−10.
(66) Klecka, G. M.; Gonsior, S. J. *Chemosphere* **1984**, *13*, 391−402.
(67) Nastainczyk, W.; Ahr, H. J.; Ullrich, V. *Biochem. Pharm.* **1982**, *31*, 391−6.
(68) Larson, R. A.; Cervini-Silva, J. *Environ. Toxicol. Chem.* **2000**, *19*, 543−548.